

Repulsive vacuum-induced forces on a magnetic particle

Kanupriya Sinha*

*Institute for Theoretical Physics, University of Innsbruck, A-6020 Innsbruck, Austria. and
Institute for Quantum Optics and Quantum Information of the Austrian Academy of Sciences, A-6020 Innsbruck, Austria.*

We study the possibility of obtaining a repulsive vacuum-induced force for a magnetic point particle near a surface. Considering the toy model of a particle with an electric-dipole transition and a large magnetic spin, we analyze the interplay between the repulsive magnetic-dipole and the attractive electric-dipole contributions to the total Casimir-Polder force. Particularly noting that the magnetic-dipole interaction is longer-ranged than the electric-dipole due to the difference in their respective characteristic transition frequencies, we find a regime where the repulsive magnetic contribution to the total force can potentially exceed the attractive electric part in magnitude for a sufficiently large spin. We analyze ways to further enhance the magnitude of the repulsive magnetic Casimir-Polder force for an excited particle, such as by preparing it in a “super-radiant” magnetic sub-level, and designing surface resonances close to the magnetic transition frequency.

I. INTRODUCTION

That the quantum fluctuations of the electromagnetic (EM) field in vacuum state can lead to forces between neutral objects is a fascinating feature of quantum electrodynamics (QED) [1]. Such fluctuation forces, often addressed by different names depending on the geometry, separation and material properties of the interacting objects, such as van der Waals [2], London [3], Casimir-Polder [4], Casimir-Lifshitz [5], or more generally Casimir [6] forces, arise as a result of the interaction mediated between the fluctuating dipole moments that constitute two neutral bodies via the quantum fluctuations of the EM field.

When considering atom-surface interactions, Casimir-Polder (CP) forces become significant in comparison to externally applied forces at distances smaller than atomic wavelengths. Being typically attractive and short-ranged, fluctuation forces are considered as a detrimental influence when trying to trap and control quantum systems near surfaces. For example, the typical magnetic and optical trap forces are easily overcome by vacuum forces at the nanoscale. As a result, when trying to interface trapped atoms with surfaces, the atoms tend to be lost from the relatively weak trapping potentials and adhere to surfaces [7].

With growing efforts towards miniaturization of photonic systems both with the fundamental motivation to explore quantum phenomena at increasingly shorter length scales, and the practical goal of replacing large-scale optical elements with modular on-chip architectures [8–14], atom-surface interactions have become an increasingly relevant aspect of understanding and designing nanoscale photonic devices. For example, Casimir interactions become an inevitable element of consideration in trapping schemes [25, 26], surface-modification of decay rates [27–30], and decoherence of atomic spins [31–33]

when trapping atoms near nanofibers [15–19], photonic crystals [20–22], micro- and nano-scale cavities [23, 24]. Thus, given that vacuum forces play an important role in state-of-the-art experiments, it is interesting to explore whether they can be engineered in a way to achieve better control and coherence of quantum systems interacting at nanoscales. Particularly, we examine here the possibility of using repulsive vacuum forces to stably trap a particle near a surface.

However, an analog of the Earnshaw’s theorem for fluctuation forces forbids stable equilibria for non-magnetic objects separated by vacuum [34]. Some possible ways to overcome this no-go theorem are [35]: going out-of-equilibrium using temperature gradients [36–38] or external drives [40], replacing the vacuum by a medium with appropriate permittivity relative to the interacting objects [41–43], using material anisotropies [44–46] and topological properties of the interacting bodies [47, 48], or designing specific geometrical configurations [49].

As another way to circumvent the no-go theorem, one can use the magnetic response of the interacting bodies [50–52]. For example, when considering the force on a magnetic atom interacting with the vacuum EM field near a perfectly conducting surface, it is known that the electric-dipole (ED) interaction between the atom and the EM field leads to an attractive CP force, while the magnetic-dipole (MD) interaction leads to a repulsive force [53, 54]. Previous works that have studied repulsive CP forces due to MD interaction between atoms and surfaces [55–57] show that the MD interaction induced repulsion is limited due to the smallness of magnetic interaction in comparison to the electric.

Keeping this in consideration, in this paper we study the possibility of using the magnetic-dipole interaction between a point-like magnetic particle with a large spin and a surface to realize an overall repulsive CP force. We find that the force due to the MD interaction has two components – a broadband Casimir-Polder contribution, and a zero frequency contribution coming from the magnetostatic interaction between the magnetic dipole and its image, which can be significant for a perfect conductor-like surface. We show that for a large enough

*Electronic address: kanupriyasinha@gmail.com

spin, in the appropriate distance regime where one has a weak short-ranged ED contribution while the MD contribution is considerable, one can have an overall repulsive vacuum-induced force. We then study two particular ways of further enhancing the magnetic CP contribution for a particle in an excited magnetic sublevel – using “superradiance”-like effects [39], and by engineering the response of the surface at the resonant frequency for the MD transition [40].

The paper is structured as follows. In section II, we present a theoretical model to describe a magnetic point particle interacting with the vacuum EM field in the presence of a surface. We study the surface-induced modifications to the internal dynamics of the atom as described by the second order Born-Markov master equation in section III. In section IV A, we analyze the force on a ground state particle with an arbitrarily large spin near a perfectly conducting surface coming from ED and MD interactions. Further, adding gravity, we study the feasibility of creating stable equilibrium by combining a repulsive magnetic force and the attractive gravitational force. In section IV B, we consider the particle near a metal surface described by Drude and plasma models. In section V, we study potential ways to preferentially enhance the repulsive magnetic CP force relative to the attractive electric CP force by considering the particle to be in an excited magnetic sublevel. We discuss the conclusions and prospects of our work in section VI.

II. MODEL

We consider a fixed magnetic point particle at the position $\mathbf{r}_0 = (0, 0, z_0)^T$ ($z_0 > 0$) placed above a planar medium that occupies the half-space $z < 0$. The half-space around the particle ($z > 0$) is assumed to be vacuum. The internal degrees of the particle consist of an electric-dipole transition between ground and excited states $|a\rangle$ and $|b\rangle$, respectively, and a magnetic spin of dimension S . We assume a classical magnetic field $\mathbf{B}_0(\mathbf{r}_0) = |\mathbf{B}_0(\mathbf{r}_0)|\mathbf{e}_z$ along the z -axis at the position of the particle. We consider the particle to be in a magnetic state $|S, m_S\rangle$, such that $\hat{\mathbf{S}}^2 |S, m_S\rangle = S(S+1) |S, m_S\rangle$, and $\hat{S}_z |S, m_S\rangle = m_S |S, m_S\rangle$, with $m_S \in \{-S, \dots, S-1, +S\}$. We note that the spin operators $(\hat{S}_x, \hat{S}_y, \hat{S}_z)$ obey the canonical commutation relations $[\hat{S}_i, \hat{S}_j] = i\epsilon_{ijk}\hat{S}_k$.

To describe the interaction between the particle and the vacuum EM field in the presence of a surface, we write the total Hamiltonian as

$$\hat{H}_{\text{tot}} = \hat{H}_P + \hat{H}_F + \hat{H}_{PF}. \quad (1)$$

The first term

$$\hat{H}_P = \hbar\omega_e\hat{\sigma}_+\hat{\sigma}_- + \hbar\omega_m\hat{S}_z, \quad (2)$$

refers to the free Hamiltonian of the particle, with ω_e as the transition frequency for the ED transition. The

ladder operators for the ED transition are defined as $\hat{\sigma}_+ \equiv |b\rangle\langle a| \otimes \mathbb{1} = (\hat{\sigma}_-)^{\dagger}$. The Zeeman splitting $\omega_m = \gamma_0|\mathbf{B}_0(\mathbf{r}_0)|$ is given by the MD interaction term $-\hat{\mathbf{m}} \cdot \mathbf{B}_0(\mathbf{r}_0) = \hbar\omega_m\hat{S}_z$, where $\hat{\mathbf{m}} = -\hbar\gamma_0\hat{\mathbf{S}}$ corresponds to the magnetic moment operator and γ_0 is the gyromagnetic ratio [58]. The Hamiltonian \hat{H}_F describing the free dynamics of the vacuum EM field in the presence of the surface is defined in Eq. (A1) [60, 61].

The interaction between the particle and the vacuum EM field in the multipolar coupling scheme, using the electric and magnetic dipole approximations, is given as [59]

$$\begin{aligned} \hat{H}_{PF} &= -\hat{\mathbf{d}} \cdot \hat{\mathbf{E}}(\mathbf{r}_0) - \hat{\mathbf{m}} \cdot \hat{\mathbf{B}}(\mathbf{r}_0), \\ &= -(\mathbf{d}\hat{\sigma}_+ + \mathbf{d}^*\hat{\sigma}_-) \cdot \hat{\mathbf{E}}(\mathbf{r}_0) \\ &\quad + \hbar\gamma_0 \left[\hat{S}_z\mathbf{e}_z + \hat{S}_+\mathbf{e}_+ + \hat{S}_-\mathbf{e}_- \right] \cdot \hat{\mathbf{B}}(\mathbf{r}_0). \end{aligned} \quad (3)$$

Here $\mathbf{d} \equiv \sqrt{2}|\langle b|\hat{\mathbf{d}}|a\rangle|\mathbf{e}_+$, $\mathbf{e}_{\pm} \equiv (\mathbf{e}_x \mp i\mathbf{e}_y)/2$, and the spin raising and lowering operators $\hat{S}_{\pm} \equiv \hat{S}_x \pm i\hat{S}_y$ are defined as

$$\hat{S}_{\pm} |S, m_S\rangle = \sqrt{S(S+1) - m_S(m_S \pm 1)} |S, m_S \pm 1\rangle. \quad (4)$$

We have assumed the ED moment to be circularly polarized for later convenience. The electric and magnetic field operators for the medium-assisted EM field, evaluated at the position of the particle, $\hat{\mathbf{E}}(\mathbf{r}_0)$ and $\hat{\mathbf{B}}(\mathbf{r}_0)$, are defined in Eq. (A4) and Eq. (A5) respectively.

III. SURFACE-INDUCED MODIFICATIONS TO THE INTERNAL DYNAMICS OF THE PARTICLE

To find the influence of the medium-assisted EM field on the particle, we derive the surface-induced modifications to the master equation describing the dynamics of the reduced density matrix $\hat{\rho}_P$, that corresponds to the internal degrees of freedom of the particle [40]. Assuming that the particle and the field are weakly coupled, and that the EM field bath correlations decay much faster than the relaxation time scale for the particle’s internal dynamics, we use the Born and Markov approximations to write the equation of motion for $\hat{\rho}_P$ as [62]

$$\begin{aligned} \frac{d\hat{\rho}_P}{dt} &= \\ &= -\frac{1}{\hbar^2} \text{Tr}_F \int_0^{\infty} d\tau \left[\tilde{H}_{PF}^{\text{sc}}(t), [\tilde{H}_{PF}^{\text{sc}}(t-\tau), \hat{\rho}_P(t) \otimes \hat{\rho}_F] \right], \end{aligned} \quad (5)$$

where $\tilde{H}_{PF}^{\text{sc}}(t) \equiv e^{-i(\hat{H}_P + \hat{H}_F)t} \hat{H}_{PF}^{\text{sc}} e^{i(\hat{H}_P + \hat{H}_F)t}$ stands for the interaction Hamiltonian in the interaction picture, including only the part of the EM field scattered off the surface, as in Eq. (A10). The reduced density matrix $\hat{\rho}_F = |0\rangle\langle 0|$ refers to that of the vacuum EM field. Tracing out the field, we obtain the surface-modifications to

the second-order Born-Markov master equation for the particle dynamics as

$$\frac{d\hat{\rho}_P}{dt} = -\frac{i}{\hbar} [\Delta\hat{H}_P, \hat{\rho}_P] + \Delta\mathcal{L}_P[\hat{\rho}_P], \quad (6)$$

where $\Delta\hat{H}_P$ corresponds to the surface-induced dispersive corrections to the particle Hamiltonian, and $\Delta\mathcal{L}_P$ refers to the surface-induced modifications to the dissipative dynamics of the particle. We remark that we have considered here only the part of the EM field scattered off the surface, without including the free-space contri-

bution that leads to the Lamb shift and the free-space dissipation.

The corrections to the particle Hamiltonian are given by,

$$\Delta\hat{H}_P = u_e^{(+)}\hat{\sigma}_+\hat{\sigma}_- + u_e^{(-)}\hat{\sigma}_-\hat{\sigma}_+ + u_m^{(+)}\hat{S}_+\hat{S}_- + u_m^{(-)}\hat{S}_-\hat{S}_+ + u_m^{(z)}\hat{S}_z^2, \quad (7)$$

The energy level shifts $u_e^{(-)}$ ($u_e^{(+)}$) in Eq. (7) to the ground (excited) state coming from the ED interaction between the particle and the field are defined as [4, 60, 61, 63, 64],

$$u_e^{(-)} = \frac{2\mu_0\omega_e|\mathbf{d}|^2}{\pi} \int_0^\infty d\xi \frac{\xi^2}{\xi^2 + \omega_e^2} (\mathbf{e}_-)^T \bar{\bar{G}}_{sc}(\mathbf{r}_0, \mathbf{r}_0, i\xi) \mathbf{e}_+, \quad (8)$$

$$u_e^{(+)} = -\frac{2\mu_0\omega_e|\mathbf{d}|^2}{\pi} \int_0^\infty d\xi \frac{\xi^2}{\xi^2 + \omega_e^2} (\mathbf{e}_+)^T \bar{\bar{G}}_{sc}(\mathbf{r}_0, \mathbf{r}_0, i\xi) \mathbf{e}_- - 2\mu_0\omega_e^2|\mathbf{d}|^2 \text{Re} \left[(\mathbf{e}_+)^T \bar{\bar{G}}_{sc}(\mathbf{r}_0, \mathbf{r}_0, \omega_e) \mathbf{e}_- \right]. \quad (9)$$

Here $\bar{\bar{G}}_{sc}(\mathbf{r}_0, \mathbf{r}_0, \omega)$, given by Eq. (B1), refers to the scattering Green's tensor corresponding to a point dipole at \mathbf{r}_0 radiating near a surface [65].

Next, we consider the shifts from the MD interaction

in Eq. (7). The energy level shifts $u_m^{(-)}$ ($u_m^{(+)}$) to the magnetic sublevels coming from the transition to the upper (lower) level, and $u_m^{(z)}$ coming from the diagonal ($\sim \hat{S}_z$) interaction term can be found as follows [56, 60, 61],

$$u_m^{(-)} = \frac{\hbar^2\mu_0\omega_m\gamma_0^2}{\pi} \int_0^\infty \frac{d\xi}{\xi^2 + \omega_m^2} (\mathbf{e}_-)^T \bar{\bar{G}}_{sc}(\mathbf{r}_0, \mathbf{r}_0, i\xi) \mathbf{e}_+, \quad (10)$$

$$u_m^{(+)} = -\frac{\hbar^2\mu_0\gamma_0^2\omega_m}{\pi} \int_0^\infty \frac{d\xi}{\xi^2 + \omega_m^2} (\mathbf{e}_+)^T \bar{\bar{G}}_{sc}(\mathbf{r}_0, \mathbf{r}_0, i\xi) \mathbf{e}_- + \mu_0\gamma_0^2 \text{Re} \left[(\mathbf{e}_+)^T \bar{\bar{G}}_{sc}(\mathbf{r}_0, \mathbf{r}_0, \omega_m) \mathbf{e}_- \right], \quad (11)$$

$$u_m^{(z)} = \frac{\hbar^2\mu_0\gamma_0^2}{2} \lim_{\xi \rightarrow 0} \left[(\mathbf{e}_z)^T \bar{\bar{G}}_{sc}(\mathbf{r}_0, \mathbf{r}_0, i\xi) \mathbf{e}_z \right], \quad (12)$$

where we have defined the double curl of the scattering Green's tensor, given by Eq. (B2), as

$$\left[\bar{\bar{G}}_{sc}(\mathbf{r}_0, \mathbf{r}_0, \omega) \right]_{il} \equiv \lim_{\mathbf{r}_1, \mathbf{r}_2 \rightarrow \mathbf{r}_0} \epsilon_{ijk} \epsilon_{nml} \frac{\partial^2}{\partial r_{1j} \partial r_{2m}} \left[\bar{G}_{sc}(\mathbf{r}_1, \mathbf{r}_2, \omega) \right]_{kn}. \quad (13)$$

The ground state shifts Eq. (8) and Eq. (10), coming purely from the energy non-conserving terms in the particle-field interaction Hamiltonian, can be attributed to the emission and reabsorption of a virtual photon scattered off the surface by the particle. The energy conserving terms lead to the excited level shifts as in Eq. (9) and Eq. (11). There are two contributions to the total excited state shifts, the first terms in Eq. (9) and Eq. (11) correspond to the off-resonant process as in the ground state shifts, wherein the particle transits from the excited to

the ground state and back, emitting and reabsorbing a virtual photon at a frequency $\omega \neq \omega_{e,m}$. In addition, the second term in Eq. (9) and Eq. (11) represents a resonant contribution that corresponds to the interaction of the particle with a real photon emitted at the resonant frequency for the ED or MD transitions.

Additionally, we note that for the MD interaction, the diagonal part of the interaction Hamiltonian that goes as $\sim \hat{S}_z$ yields an energy shift $u_m^{(z)}$, as given in Eq. (12). Such a term is non-vanishing only for a surface with a non-zero response at static frequencies, for example, a perfect conductor. This contribution can be thus understood in terms of a static component of the magnetic dipole interacting with its image such that the normal component of the B field at the surface vanishes [66–68]. We consider this static contribution to the magnetic level shift as separate from the fluctuation-induced CP poten-

tials in Eq. (8)–Eq. (11).

Considering the Liouvillian part of the master equation, we can write the modification to the dissipative dynamics of the internal levels of the particle as follows

$$\begin{aligned} \Delta\mathcal{L}_P[\hat{\rho}_P] = & \frac{\Delta\Gamma_e}{2} [2\hat{\sigma}_-\hat{\rho}_P\hat{\sigma}_+ - \hat{\sigma}_+\hat{\sigma}_-\hat{\rho}_P - \hat{\rho}_P\hat{\sigma}_+\hat{\sigma}_-] \\ & + \frac{\Delta\Gamma_m}{2} [2\hat{S}_-\hat{\rho}_P\hat{S}_+ - \hat{S}_+\hat{S}_-\hat{\rho}_P - \hat{\rho}_P\hat{S}_+\hat{S}_-], \end{aligned} \quad (14)$$

where the corrections to the dissipation rates for the excited states are given as

$$\Delta\Gamma_e = \frac{4\mu_0\omega_e^2|\mathbf{d}|^2}{\hbar} \text{Im} \left[(\mathbf{e}_+)^T \bar{\bar{G}}_{\text{sc}}(\mathbf{r}_0, \mathbf{r}_0, \omega_e) \mathbf{e}_- \right], \quad (15)$$

$$\Delta\Gamma_m = -\frac{2\hbar\mu_0\gamma_0^2}{\hbar} \text{Im} \left[(\mathbf{e}_+)^T \bar{\bar{G}}_{\text{sc}}(\mathbf{r}_0, \mathbf{r}_0, \omega_m) \mathbf{e}_- \right]. \quad (16)$$

Here $\Delta\Gamma_e$ refers to the correction to the dissipation for the excited state $|b\rangle$, and $\Delta\Gamma_m(\langle S, m_S | \hat{S}^+ \hat{S}^- | S, m_S \rangle)$ is the modified spin flip rate for transition between the mag-

netic sublevel $|S, m_S\rangle \rightarrow |S, m_S - 1\rangle$ in the presence of the surface [31–33].

IV. CASIMIR-POLDER FORCE ON A GROUND STATE MAGNETIC PARTICLE

Having obtained the general expressions for the surface-induced dispersive Eq. (8)–Eq. (12) and dissipative Eq. (15)–Eq. (16) corrections to the particle dynamics, we now consider a particle in the ground state $|a, S, m_S = -S\rangle$ placed near a planar surface, and study the resulting vacuum-induced forces.

The level shift for the ground state can be written as

$$\langle a, S, -S | \Delta\hat{H}_P | a, S, -S \rangle = U_e^{(-)} + U_m^{(-)} + U_m^{(z)}, \quad (17)$$

where we have defined $U_e^{(-)} \equiv u_e^{(-)}$, $U_m^{(-)} \equiv Su_m^{(-)}$, $U_m^{(z)} \equiv S^2u_m^{(z)}$. Using the Green's tensor for a point dipole near a planar surface, as defined in Eq. (B1) and Eq. (B2), one obtains

$$U_e^{(-)} = \frac{3\hbar\Gamma_0}{8\pi} \int_0^\infty \frac{d\xi}{\omega_e} \frac{\xi^2}{\xi^2 + \omega_e^2} \int_{\xi/c}^\infty \frac{d\kappa_\perp}{k_e} e^{-2\kappa_\perp z_0} \left[r_s(\kappa_\perp, i\xi) - r_p(\kappa_\perp, i\xi) \frac{\kappa_\perp^2 c^2}{\xi^2} \right], \quad (18)$$

$$U_m^{(-)} = \frac{3\hbar\Gamma_0}{8\pi} \tilde{\omega}\eta S \int_0^\infty \frac{d\xi}{\omega_e} \frac{\xi^2}{\xi^2 + \omega_m^2} \int_{\xi/c}^\infty \frac{d\kappa_\perp}{k_e} e^{-2\kappa_\perp z_0} \left[r_p(\kappa_\perp, i\xi) - r_s(\kappa_\perp, i\xi) \frac{\kappa_\perp^2 c^2}{\xi^2} \right], \quad (19)$$

$$U_m^{(z)} = -\frac{3\hbar\Gamma_0}{8} \eta S^2 \lim_{\xi \rightarrow 0} \int_{\xi/c}^\infty \frac{d\kappa_\perp}{k_e} e^{-2\kappa_\perp z_0} \frac{1}{k_e^2} \left(\kappa_\perp^2 + \frac{\xi^2}{c^2} \right) r_s(\kappa_\perp, i\xi). \quad (20)$$

Here $\Gamma_0 \equiv |\mathbf{d}|^2 k_e^3 / (3\pi\epsilon_0\hbar)$ refers to the spontaneous emission rate for the ED transition in free space, $\tilde{\omega} \equiv \omega_m/\omega_e$, $k_e \equiv \omega_e/c$, and $r_{s,p}$ are the Fresnel coefficients (see Eq. (B3)) for the field reflecting off the planar half space that include the surface material properties. We define the characteristic magnetizability to polarizability parameter as

$$\eta \equiv \frac{\hbar^2\gamma_0^2}{|\mathbf{d}|^2 c^2} = \frac{\alpha^2}{|\mathbf{d}|^2 / (\epsilon a_0)^2}, \quad (21)$$

with α as the fine-structure constant, e as the electronic charge and a_0 as the Bohr radius. The parameter η determines the characteristic strength of the magnetic to electric CP potential, thus playing a key role in deciding the overall sign of the CP force. It can be seen from Eq. (19) and Eq. (20) that the effective strength of the total magnetic potential has a factor of S for the off-resonant interaction term, and S^2 for the diagonal \hat{S}_z term in the interaction Hamiltonian. The latter contributes only for surfaces with a non-vanishing static frequency response [66], and the scaling of the potential as $\sim S^2$ can be understood in terms of the magnetostatic interaction of the

dipole with its image.

By rewriting the electric and magnetic dipole moments for the particle in terms of a corresponding polarizability, the foregoing analysis is generally applicable to a magnetic particle that can be described as a point electric and magnetic dipole near a planar surface, such as a nanosphere with a radius smaller than other relevant length scales in the problem [69]. The electric and magnetic polarizability tensors for the magnetic particle in its ground state can be written as follows [60]

$$\bar{\bar{\alpha}}_e(\omega) = \frac{|\mathbf{d}|^2 \omega_e}{\hbar(\omega_e^2 - \omega^2)} \mathbf{e}_+ \mathbf{e}_-, \quad (22)$$

$$\bar{\bar{\alpha}}_m(\omega) = \frac{2\hbar\omega_m\gamma_0^2 S}{\omega_m^2 - \omega^2} \mathbf{e}_+ \mathbf{e}_- + \pi\hbar\gamma_0^2 S^2 \delta(\omega) \mathbf{e}_z \mathbf{e}_z. \quad (23)$$

We note that the static electric polarizability can be related to the free space spontaneous emission as $\alpha_e(0) = 3\pi\epsilon_0\Gamma_0 / (k_e^4 c)$.

A. Ground state particle near a perfect conductor

For the case of a particle placed near a perfect conductor, such that the reflection coefficients are $r_p = 1$ and $r_s = -1$ [60], the level shifts Eq. (18), Eq. (19) and Eq. (20) can be written as

$$\tilde{U}_e^{(-)} = -\frac{3}{32\pi\tilde{z}^3} \int_0^\infty \frac{d\xi \omega_e}{\xi^2 + \omega_e^2} f\left(\frac{2\xi z_0}{c}\right), \quad (24)$$

$$\tilde{U}_m^{(-)} = \frac{3}{32\pi\tilde{z}^3} \eta S \int_0^\infty \frac{d\xi \omega_m}{\xi^2 + \omega_m^2} f\left(\frac{2\xi z_0}{c}\right), \quad (25)$$

$$\tilde{U}_m^{(z)} = \frac{3}{32\tilde{z}^3} \eta S^2. \quad (26)$$

We have defined the dimensionless particle-surface distance $\tilde{z} \equiv k_e z_0$, the dimensionless potentials $\tilde{U}_{e,m}^{(\pm,z)} \equiv U_{e,m}^{(\pm,z)}/(\hbar\Gamma_0)$, and $f(x) \equiv (1+x+x^2)e^{-x}$. As an important point, we note that while the electric CP potential is attractive, the magnetic CP potential is repulsive. This can be understood from the method of images in electromagnetism, since an electric dipole placed near an infinite planar perfect conductor is attracted towards its image, while a magnetic dipole experiences a repulsive force [4, 70]. We further note that the static contribution to the magnetic level shift Eq. (26) coincides with the energy of a static magnetic dipole interacting with its image near a perfectly conducting planar surface [68].

We consider the CP potentials $U_{e,m}^{(-)}$ in two asymptotic limits depending on the particle-surface distance relative to the characteristic length scales for ED and MD interactions. For example, in the non-retarded limit where $z_0 \ll c/\omega_{e(m)}$, the corresponding electric (magnetic) CP potential interaction scales as $\sim 1/z_0^3$. In the retarded limit, given by $z_0 \gg c/\omega_{e(m)}$, the electric (magnetic) CP potential scales as $\sim 1/z_0^4$. Further assuming that $\omega_e \gg \omega_m$ ¹, one can define the three regimes depicted in Table I as follows.

- Region I, defined by $z_0 \ll c/\omega_{e,m}$, wherein both the electric and magnetic CP forces are non-retarded (NR), and defined as

$$\begin{aligned} \tilde{U}_e^{(\text{NR})} &\equiv \lim_{z_0 \ll c/\omega_e} \tilde{U}_e^{(-)}, \\ \tilde{U}_m^{(\text{NR})} &\equiv \tilde{U}_m^{(z)} + \lim_{z_0 \ll c/\omega_m} \tilde{U}_m^{(-)}. \end{aligned} \quad (27)$$

- Region III, defined by $z_0 \gg c/\omega_{e,m}$ such that both the electric and magnetic CP potentials are re-

tarded (R), such that

$$\begin{aligned} \tilde{U}_e^{(\text{R})} &\equiv \lim_{z_0 \gg c/\omega_e} \tilde{U}_e^{(-)}, \\ \tilde{U}_m^{(\text{R})} &\equiv \tilde{U}_m^{(z)} + \lim_{z_0 \gg c/\omega_m} \tilde{U}_m^{(-)}. \end{aligned} \quad (28)$$

- Region II, defined by $c/\omega_e \ll z_0 \ll c/\omega_m$ such that the electric CP potential is retarded (R), while the magnetic CP potential is non-retarded (NR).

The CP potentials in these asymptotic limits are given in Table I.

Let us define the dimensionless total force on the particle as

$$\tilde{\mathcal{F}}_{\text{tot}} = \tilde{\mathcal{F}}_V + \tilde{\mathcal{F}}_G, \quad (29)$$

where $\tilde{\mathcal{F}}_V$ refers to the vacuum-induced force and $\tilde{\mathcal{F}}_G$ to the gravitational force, assumed along the negative z -direction. Assuming the mass of the particle to be $M = Sm_u$, where $m_u \approx 1.66 \times 10^{-27}$ kg refers to the atomic mass unit, the dimensionless gravitational force is defined as $\tilde{\mathcal{F}}_G \equiv -Mg/(\hbar\Gamma_0 k_e)$, g being the acceleration due to gravity.

The dimensionless vacuum-induced force due to the ED and MD interactions is given by $\tilde{\mathcal{F}}_V \equiv \tilde{\mathcal{F}}_e^{(-)} + \tilde{\mathcal{F}}_m^{(-)} + \tilde{\mathcal{F}}_m^{(z)}$, where $\tilde{\mathcal{F}}_{e,m}^{(j)} \equiv -\partial\tilde{U}_{e,m}^{(j)}/\partial\tilde{z}$. We further define the total force excluding the magnetostatic contribution as the sum of the CP forces and gravity

$$\tilde{\mathcal{F}}_{\text{tot}}^{\text{CP}} \equiv \tilde{\mathcal{F}}_e^{(-)} + \tilde{\mathcal{F}}_m^{(-)} + \tilde{\mathcal{F}}_G, \quad (30)$$

which is relevant for surfaces with a vanishing static frequency response.

In the following, we analyze the total force with and without the magnetostatic contribution as given by Eq. (29) and Eq. (30) respectively. For estimate purposes, we choose $\omega_e = 2\pi \times 10^{15}$ Hz, $\omega_m = 2\pi \times 10^{10}$ Hz, and $\Gamma_0 = 18$ MHz, which corresponds to an ED moment value of $|\mathbf{d}| \approx ea_0/2$.

- Casimir-Polder repulsion (excluding magnetostatic contribution): The threshold value of the spin to facilitate an overall repulsive CP force, given by Eq. (30), in the region I is roughly given as

$$\eta S_0^{\text{CP}} \approx 1, \text{ or } S_0^{\text{CP}} \approx 10^4, \quad (31)$$

as can be seen from Fig. 1(a). Thus, the condition $S \gtrsim S_0^{\text{CP}}$ defines a key constraint for achieving near-field CP repulsion for a magnetic particle in the ground state. In the retarded regime (region III), the condition for having a repulsive CP force becomes

$$\eta S \gtrsim \tilde{\omega}, \quad (32)$$

as seen from Fig. 1(a). This can be readily realized for $\tilde{\omega} \lesssim 10^{-4}$, thus yielding a repulsive force in the far-field limit.

¹ We restrict our attention here to magnetic dipole transitions within a single electronic level, which typically occur at microwave or radio frequencies, unlike optical magnetic dipole transitions [71] that can occur between different electronic levels.

For $S > S_0^{\text{CP}}$, approximating the total force as $\tilde{\mathcal{F}}_{\text{tot}}^{\text{CP}} \approx \tilde{\mathcal{F}}_m^{(-)} + \tilde{\mathcal{F}}_G$, the position for having a stable equilibrium is given as

$$\tilde{z}_{\text{eq}}^{\text{CP}} = \left(\frac{9\eta\hbar\Gamma_0 k_e}{64m_u g} \right)^{1/4}. \quad (33)$$

We note that with both the repulsive magnetic CP ($\tilde{\mathcal{F}}_m^{(-)}$) and attractive gravitational ($\tilde{\mathcal{F}}_G$) contributions to the total force scaling as $\sim S$, the equilibrium position is independent of the spin, as seen from the dotted vertical line in Fig. 1(b). It can be also verified from Fig. 1(a), that the gravitational force becomes comparable in magnitude to the magnetic CP force for $\tilde{z} \approx \tilde{z}_{\text{eq}}^{\text{CP}}$.

- Total vacuum-induced repulsion (including magnetostatic contribution): Considering the total vacuum-induced force along with gravity, as defined in (29), we see from Table I that to achieve a repulsive near-field total force one requires $\eta S(2S+1) \gtrsim 1$. Assuming that $|\mathbf{d}| \approx ea_0/2$, we obtain a threshold spin value of

$$S_0 \approx \sqrt{1/(2\eta)}, \text{ or } S_0 \approx 50, \quad (34)$$

for near field repulsion.

For $S > S_0$, the total force can be well-approximated by $\tilde{\mathcal{F}}_{\text{tot}} \approx \tilde{\mathcal{F}}_m^{(z)} + \tilde{\mathcal{F}}_G$, such that with the near-field magnetostatic repulsion and far-field gravitational attraction, one obtains a stable equilibrium point

$$\tilde{z}_{\text{eq}} \approx \left(\frac{9\eta S \hbar \Gamma_0 k_e}{32m_u g} \right)^{1/4}. \quad (35)$$

We note from the above that the equilibrium point gets pushed away from the surface on increasing the spin value S .

We have discussed here the general conditions and parameter regimes for realizing a repulsive force between a ground state magnetic particle and a perfectly conducting planar surface using MD interaction and the possibility of levitating it against gravity. In the following section we study how these conditions generalize for the particle placed near more realistic metal surface described by the Drude or plasma model.

B. Ground state particle near metal surfaces

The dielectric permittivity of a metal can be modeled by the Drude or plasma models as described by the permittivity functions as in Eq. (36) and Eq. (41) respectively. The key difference in the two models is that the plasma model disregards the relaxation of conducting electrons in the metal. This difference matters the most

for the low frequency response of the metals, and can lead to very different resulting Casimir forces [72–74]. Such a discrepancy has been much debated in the literature, with the experimental results favoring the plasma model in some cases, and Drude in others [75–81].

Particularly, the response of the metal at zero frequency is largely different between the two models. For example, while the Fresnel coefficient $r_s(\kappa_\perp, 0) \rightarrow 0$ for the Drude model, it is non-vanishing for the plasma model [74]. As we have seen from Eq. (20), the Fresnel coefficient $r_s(\kappa_\perp, 0)$ is crucial for determining the magnetostatic contribution. Thus, for a ground state particle, given that \hat{S}_z term contribution scales as $\sim S^2$, as opposed to the broadband CP contribution that scales as $\sim S$ (see Eq. (17)), the two models for the dielectric permittivity of the metal could yield a very different magnetic force for a large enough spin system. In the following sections we study the conditions for achieving an overall repulsive force from the ED and MD interactions near a metal surface described by the Drude and plasma model, particularly noting the difference in the two results due to the magnetostatic contribution.

1. Drude model

Considering a metal surface with a Drude model for dielectric permittivity

$$\epsilon_D(i\xi) = 1 + \frac{\omega_p^2}{\xi^2 + \gamma\xi}, \quad (36)$$

where ω_p is the plasma frequency of the metal and $\gamma \ll \omega_p$ corresponds to the loss. Using the above dielectric permittivity for the optical response of the surface, one can find the ground state level shifts as given by Eq. (18) and Eq. (19). Assuming $\omega_{p,e} \gg \omega_m$ [56], there are three limiting cases of the resulting level shifts as summarized in Table I. In region (I) III, both the ED and MD interaction induced level shifts are in the (non-)retarded limit. In addition to the retarded and non-retarded regimes, there is a separate length scale in the problem that corresponds to the plasma frequency of the metal. This leads to a different asymptotic behaviour for the magnetic level shift in the intermediate regime demarcated by $c/\omega_p \ll z_0 \ll c/\omega_m$, defined as

$$\tilde{U}_m^{\text{Int}} \equiv \tilde{U}_m^{(z)} + \lim_{c/\omega_p \ll z_0 \ll c/\omega_m} \tilde{U}_m^{(-)}. \quad (37)$$

We note that in the retarded limit the metal surface behaves as a perfect conductor, as far as the electric level-shift is concerned. This can be physically understood by considering that the relevant frequencies for the far-field interaction being small, the plasma frequency of the metal appears infinite, which corresponds to the response of a perfect conductor.

Importantly, it can be seen from Eq. (B3) that with $\lim_{\xi \rightarrow 0} r_s(\kappa_\perp, i\xi) = 0$, the static contribution as given

	Perfect conductor	Drude model	Plasma model
I. $z_0 \ll c/\omega_{e,p,m}$	$\tilde{U}_e^{\text{NR}} \approx -\frac{3}{64\tilde{z}^3}$ $\tilde{U}_m^{\text{NR}} \approx \frac{3}{64\tilde{z}^3}\eta S(2S+1)$	$\tilde{U}_e^{\text{NR}} \approx \frac{C_{e,D}^{(3)}}{\tilde{z}^3}$ $\tilde{U}_m^{\text{NR}} \approx \frac{C_{m,D}^{(1)}}{\tilde{z}}$	$\tilde{U}_e^{\text{NR}} \approx \frac{C_{e,D}^{(3)}}{\tilde{z}^3}$ $\tilde{U}_m^{\text{NR}} \approx \frac{C_{m,P}^{(1)}}{\tilde{z}}$
II. $c/\omega_{e,p} \ll z_0 \ll c/\omega_m$	$\tilde{U}_e^{\text{R}} \approx -\frac{3}{16\pi\tilde{z}^4}$ $\tilde{U}_m^{\text{NR}} \approx \frac{3}{64\tilde{z}^3}\eta S(2S+1)$	$\tilde{U}_e^{\text{R}} \approx -\frac{3}{16\pi\tilde{z}^4}$ $\tilde{U}_m^{\text{Int}} \approx \frac{3}{64\tilde{z}^3}\eta S$	$\tilde{U}_e^{\text{R}} \approx -\frac{3}{16\pi\tilde{z}^4}$ $\tilde{U}_m^{\text{Int}} \approx \frac{3}{64\tilde{z}^3}\eta S(2S+1)$
III. $c/\omega_{e,p,m} \gg z_0$	$\tilde{U}_e^{\text{R}} \approx -\frac{3}{16\pi\tilde{z}^4}$ $\tilde{U}_m^{\text{R}} \approx \frac{3}{16\pi\tilde{z}^4}\frac{\eta S}{\tilde{\omega}}\left(\frac{\pi S\tilde{z}\tilde{\omega}}{2}+1\right)$	$\tilde{U}_e^{\text{R}} \approx -\frac{3}{16\pi\tilde{z}^4}$ $\tilde{U}_m^{\text{R}} \approx \frac{3}{16\pi\tilde{z}^4}\frac{\eta S}{\tilde{\omega}}$	$\tilde{U}_e^{\text{R}} \approx -\frac{3}{16\pi\tilde{z}^4}$ $\tilde{U}_m^{\text{R}} \approx \frac{3}{16\pi\tilde{z}^4}\frac{\eta S}{\tilde{\omega}}\left(\frac{\pi S\tilde{z}\tilde{\omega}}{2}+1\right)$

TABLE I: Energy level shifts for a magnetic particle in the ground state $|a, S, m_S = -S\rangle$ placed near a (1) perfectly conducting planar surface, and a metal surface described by the (2) Drude, and (3) plasma models for dielectric permittivity. The level shifts in (non-)retarded asymptotic limits are defined as in Eq. (27) and Eq. (28). For the Drude and plasma models, there being a separate length scale corresponding to the plasma frequency of the surface, there is a different asymptotic behavior for the magnetic CP potential in the intermediate distance regime where one is in the non-retarded limit relative to the MD transition frequency but retarded relative to the plasma frequency of the surface ($c/\omega_p \ll z_0 \ll c/\omega_m$), as defined in Eq. (37). It can be seen that in the retarded limit, the level shifts for the plasma (Drude) model mimic those for the perfect conductor, with (without) the static frequency contribution, since in the far-field limit the response of the metal surface at low frequencies corresponds to that of a perfect conductor. The coefficients C_j^k for Drude and plasma models are defined in Eq. (C5)–Eq. (C7).

by Eq. (20) vanishes, such that the total magnetic CP potential is given as

$$\tilde{U}_m^{(-)} = \frac{3}{8\pi}\tilde{\omega}\eta S \int_0^\infty \frac{d\xi}{\omega_e} \frac{\xi^2}{\xi^2 + \omega_m^2} \int_{\xi/c}^\infty \frac{d\kappa_\perp}{k_e} e^{-2\kappa_\perp z_0} \left[r_p(\kappa_\perp, i\xi) - r_s(\kappa_\perp, i\xi) \frac{\kappa_\perp^2 c^2}{\xi^2} \right], \quad (38)$$

which can be calculated in the three asymptotic limits using the approach in Appendix C, as summarized in Table I. Specifically, we note here that the above potential scales linearly with the total spin S , in contrast to the case of a perfect conductor.

It can be seen from Table I, that for the total CP force to be repulsive in region I, one requires

$$\left| \frac{\tilde{U}_m^{\text{NR}}}{\tilde{U}_e^{\text{NR}}} \right| \approx \frac{C_{m,D}^{(1)}}{C_{e,D}^{(3)}} \tilde{z}^2 \sim \eta S \frac{\omega_p^2}{\omega_e^2} \frac{\ln(\gamma/\omega_m)}{\gamma/\omega_m} \tilde{z}^2, \quad (39)$$

with the coefficients $C_{m,D}^{(1)}$ and $C_{e,D}^{(3)}$ given by Eq. (C6) and Eq. (C5), assuming $\omega_p \sim 100\gamma \sim 10\omega_e \sim 10^7\omega_m$. Considering the particle near a gold surface with $\omega_p \approx$

1.36×10^{16} Hz and $\gamma \approx 10^{14}$ Hz, one requires

$$\eta S \gtrsim \frac{10^3}{\tilde{z}^2}, \quad (40)$$

for the total CP force in region I to be repulsive. For a particle-surface separation $z_0 \approx 10$ nm, we find that one requires the total spin to be as large as $S \gtrsim 10^8$ to achieve repulsion.

2. Plasma model

We now consider the plasma model for dielectric permittivity, by setting the relaxation parameter in the

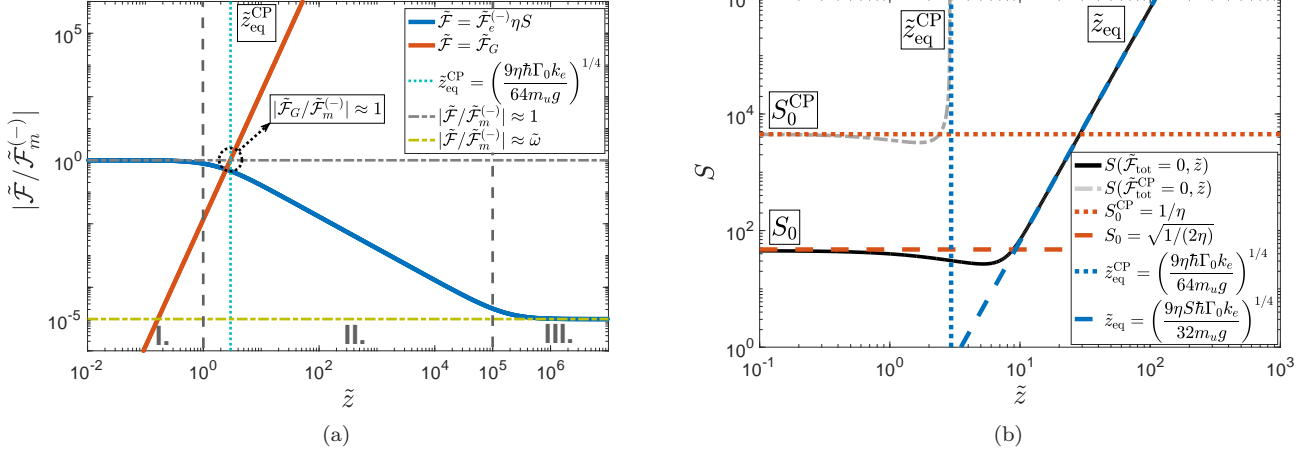


FIG. 1: (a) Relative magnitudes of the rescaled electric CP force (blue solid) and gravity (red solid) compared to the magnetic CP force on a ground state particle as a function of distance. The three distance regimes as shown in Table I are depicted as the dashed gray vertical lines. In region I (III), the electric and magnetic CP forces are such that $\tilde{\mathcal{F}}_m^{(-)}/\tilde{\mathcal{F}}_e^{(-)} \approx \eta S$ ($\tilde{\mathcal{F}}_m^{(-)}/\tilde{\mathcal{F}}_e^{(-)} \approx \eta S/\tilde{\omega}$), yielding the condition given by Eq. (31) (Eq. (32)) for near-(far)-field Casimir repulsion. For a large enough spin, the condition $|\tilde{\mathcal{F}}_G/\tilde{\mathcal{F}}_m^{(-)}| \approx 1$ defines the condition for achieving a stable equilibrium, as shown by the intersection point for the red solid and gray dashed-dotted curves. It can be seen that this point coincides with the approximate analytical expression obtained in Eq. (33) as depicted by the vertical blue dotted line. (b) Spin value $S(\tilde{\mathcal{F}}_{\text{tot}}^{(\text{CP})} = 0, \tilde{z})$ as a function of the particle-surface distance \tilde{z} for the total force $\tilde{\mathcal{F}}_{\text{tot}}^{(\text{CP})}$ with(out) the magnetostatic contribution to be zero shown in black solid (gray dashed-dotted) curve. The threshold spin value $S_0^{(\text{CP})}$ for near field repulsion defined by (Eq.(31)) Eq.(34) is shown by the red (dotted) dashed line. The approximate stable equilibrium point given by (Eq. (33)) Eq. (35) are shown in blue (dotted) dashed curve.

Drude model to zero

$$\epsilon_P(i\xi) = 1 + \frac{\omega_p^2}{\xi^2}. \quad (41)$$

Using the above dielectric response in Eq. (18) and Eq. (19), one can find the ED and MD interaction induced potentials in the three asymptotic limits as outlined in Table I. In the near-field limit, one can thus write the ratio of the repulsive magnetic potential to the attractive electric part as

$$\left| \frac{\tilde{U}_m^{\text{NR}}}{\tilde{U}_e^{\text{NR}}} \right| \approx \frac{\mathcal{C}_{m,P}^{(1)}}{\mathcal{C}_{e,D}^{(3)}} \tilde{z}^2 \sim \eta S (2S + 1) \frac{\omega_p^2}{\omega_e^2} \tilde{z}^2, \quad (42)$$

where the coefficients $\mathcal{C}_{m,P}^{(1)}$ and $\mathcal{C}_{m,D}^{(3)}$ are given by Eq. (C7) and Eq. (C5) respectively, assuming $\omega_p \sim 10\omega_e \sim 10^7\omega_m$. Again, considering the particle near a gold surface with $\omega_p \approx 1.36 \times 10^{16}$ Hz, one requires

$$\eta S (2S + 1) \gtrsim \frac{10^{-2}}{\tilde{z}^2}, \quad (43)$$

which yields, assuming a particle-surface separation of $z_0 = 10$ nm, a spin value of $S \gtrsim 10^2$ for the total force in the near-field regime to be repulsive. Thus, we see that one requires a much smaller spin value to achieve an

overall repulsive force for a particle near a metal surface if the surface response at zero frequency is described by the plasma model as opposed to the Drude model. Further, comparing Eq. (39) and Eq. (42), we see that the repulsive magnetic level shift is for the Drude model relative to the plasma model is smaller by a factor $\sim \omega_m/(S\gamma)$.

Considering that one requires spin values as large as $S \sim 10^8$ to achieve an overall repulsive CP force near a metal surface described by the Drude model, we further propose some possible ways to boost the repulsive magnetic contribution to the total CP force in the following section.

V. CASIMIR-POLDER FORCE ON AN EXCITED MAGNETIC PARTICLE

As discussed in section II, for a particle in the ground state, its only possible interactions with the field are via virtual excitation processes that can occur at all frequencies, making the interaction essentially broadband. However, for an particle in the excited state, there can be a real transition to lower energy states accompanied by the emission of a real photon, which yields a resonant shift to the excited state and modifies the dissipation rate in the presence of a surface. With the resonant shift depending singularly on the response of the surface at the transi-

tion frequency of the particle as opposed to a broadband response, as a result the excited state shifts can be manipulated relatively easily by altering the density of field modes at the transition frequency [40].

In addition, we further note from Eq. (7) (and Eq. (4)) that if we consider the magnetic particle to be in the excited level $|S, m_S = 0\rangle$, the characteristic strength for the magnetic CP interaction (excluding the static contribution) is larger by a factor of S in comparison to that for the ground state. Drawing the analogy between a spin system and the Dicke model [82, 83], such an enhancement can be understood as that in the case of superradiance in a collection of atoms. In the case of Dicke superradiance, the enhancement in the transition amplitude for the superradiant state corresponding to $|S, m_S = 0\rangle$ leads to a boost by a factor of S in the collective spontaneous emission rate of the atoms. Since the CP force is also a fluctuation phenomenon, one can naturally expect that the cooperative effects that influence the spontaneous emission for a collection of atoms to also influence the CP force [39, 84].

Thus, given that (i) the excited state shifts depend on the response of the surface at the resonant transition frequency, such that one can enhance the repulsive magnetic CP potential by appropriately engineering the surface response, and (ii) that by preparing the particle in an excited state one can further boost the repulsive magnetic CP force, we therefore consider the CP interaction for a particle in the state $|a, S, m_S = 0\rangle$. We analyze these two effects in the following.

A. The magnetic CP potential for the excited sublevel $|S, m_S = 0\rangle$

The total level shift of the state $|S, m_S = 0\rangle$ comprises of three contributions. First, there is an off-resonant contribution from the virtual transition to the level $|S, m_S = +1\rangle$ as described by Eq. (10). Next, considering the transition to the level $|S, m_S = -1\rangle$ there is an off-resonant and a resonant contribution as seen from the first and second terms in Eq. (11) respectively.

Adding together the contributions from the transition to the levels $|S, m_S = \pm 1\rangle$ using Eq. (11) and Eq. (10), we find the total magnetic CP shift on the level $|S, m_S = 0\rangle$ for a particle near a planar surface ,

$$\tilde{U}_m^{(0)} = -\frac{3\eta S(S+1)\tilde{\omega}^3}{16} \text{Re} \int_0^\infty \frac{dk_{\parallel}}{k_m} \frac{k_{\parallel}}{\kappa_{\perp}} e^{-2\kappa_{\perp}z_0} \left[r_p(\kappa_{\perp}, \omega_m) + r_s(\kappa_{\perp}, \omega_m) \frac{\kappa_{\perp}^2}{k_m^2} \right]. \quad (44)$$

Comparing the above with the broadband contribution in Eq. (19), the magnetizability to polarizability for the $|S, m_S = 0\rangle$ level is larger by an additional factor of S with respect to the ground state. We also note that for $m_S = 0$, the contribution from the diagonal interaction term in Eq. (20) vanishes.

Considering the particle placed near a perfectly conducting surface, we write the magnetic CP potential for the state $|a, S, m_S = 0\rangle$ as

$$\tilde{U}_m^{(0)} = \frac{3\eta S(S+1)}{64\tilde{z}^3} [\cos(2\tilde{\omega}\tilde{z}) + 2\tilde{\omega}\tilde{z}\sin(2\tilde{\omega}\tilde{z}) - 4\tilde{\omega}^2\tilde{z}^2\cos(2\tilde{\omega}\tilde{z})]. \quad (45)$$

In the non-retarded regime for the magnetic CP potential ($\tilde{\omega}\tilde{z} \ll 1$), the above potential reduces to $\tilde{U}_m^{(0),\text{NR}} \approx 3\eta S(S+1)/(64\tilde{z}^3)$. Thus for the total CP force to be repulsive in the near-field regime such that $\tilde{U}_e^{\text{NR}} + \tilde{U}_m^{(0),\text{NR}} > 0$, one requires $\eta S(S+1) \gtrsim 1$, or $S \gtrsim 10^2$.

Adding together the CP force and gravity as before, the total potential in the near-field regime (considering $S \gtrsim 10^2$) can be described approximately as the sum of the non-retarded magnetic CP potential and the gravitational potential as

$$\tilde{\mathcal{F}}_{\text{tot}}^{\text{approx}} \approx \frac{9\eta S(S+1)}{64\tilde{z}^4} - \frac{Mg}{\hbar\Gamma_0 k_e}. \quad (46)$$

Thus there is a stable equilibrium point along the z -direction at

$$\tilde{z}_{\text{eq}}^{(0)} \approx \left(\frac{9\eta S \hbar \Gamma_0 k_e}{64 m_u g} \right)^{1/4}, \quad (47)$$

where the attractive gravitational force balances the magnetic repulsion. We see that on increasing S , the magnetic repulsion increases more than the gravitational attraction and the equilibrium point gets pushed further away from the surface.

The modified spin-flip rate given by Eq. (16) in the non-retarded limit is given as $\Delta\Gamma_m^{(0),\text{NR}} \approx \Gamma_0 \eta S(S+1)\tilde{\omega}^3/3 \sim 10^{-9}$ Hz [31–33], considering a spin value of $S = 100$. In the absence of surface losses, the decay rate is independent of the particle-surface separation in the non-retarded limit, as expected from image theory [63].

In the following section we study the possibility of combining such a “super-radiant” enhancement to the repulsive CP force together with an additional boost coming from surface resonance for a particle placed near a metal surface described by the Drude model.

B. Enhancing the magnetic CP force using surface resonances

It can be seen from Eq. (44) that the off-resonant shift contribution from the virtual transition to the level $|S, m_S = +1\rangle$ cancels with that to the level $|S, m_S = -1\rangle$, as expected from second-order perturbation theory, such that the overall magnetic shift on the $|S, m_S = 0\rangle$ level contains only the resonant contribution. As a result, the total magnetic CP potential depends singularly on the response of the surface at the resonant transition frequency ω_m . Thus, we consider here the possibility of boosting

the magnetic CP force resonantly by engineering the response of the surface at ω_m following the approach in [40].

Modeling the surface response using the Drude model given by Eq. (36), one can see from Eq. (44) and Eq. (B3) that in order to find the CP potential one only requires the dielectric response of the surface at the resonance transition frequency $\epsilon_m \equiv \epsilon(\omega_m)$ (assuming $\mu(\omega_m) = 1$). In the non-retarded limit for MD interaction ($\tilde{\omega}\tilde{z} \ll 1$), we use the approach in Appendix C to write an asymptotic expression for the non-retarded magnetic CP potential near a metal surface as

$$\tilde{U}_m^{(0),\text{NR}} \approx \frac{3\eta S(S+1)\tilde{\omega}^2}{128\tilde{z}} \text{Re} \left[\frac{(\epsilon_m - 1)(\epsilon_m + 5)}{\epsilon_m + 1} \right]. \quad (48)$$

The above potential undergoes a resonance for $(\epsilon_m + 1) \rightarrow 0$ near the plasmon resonance given by $\omega_m \rightarrow \omega_p/\sqrt{2}$. We define the quality factor for the surface material as $Q \equiv \omega_p/(\sqrt{2}\gamma)$, and the dimensionless detuning with respect to the plasmon resonance as $\delta_p \equiv (\omega_m - \omega_p/\sqrt{2})/\gamma$. Assuming a high Q-factor for surface resonance and large detuning such that $Q \gg |\delta_p| \gg 1$, one can rewrite the non-retarded magnetic CP potential as

$$\tilde{U}_m^{(0),\text{NR}} \approx -\frac{3\eta S(S+1)\tilde{\omega}^2}{256\tilde{z}} \left(\frac{Q}{\delta_p} \right). \quad (49)$$

The ratio of the magnetic to electric CP potential given by Eq. (C5) in region I goes roughly as,

$$\left| \frac{\tilde{U}_m^{(0),\text{NR}}}{\tilde{U}_e^{\text{NR}}} \right| \sim \eta S(S+1)\tilde{\omega}^2\tilde{z}^2 \left(\frac{Q}{|\delta_p|} \right), \quad (50)$$

such that to achieve near field repulsion we require

$$\eta S(S+1) \gtrsim \frac{1}{\tilde{\omega}^2\tilde{z}^2} \left(\frac{|\delta_p|}{Q} \right). \quad (51)$$

For a particle-surface distance of $z_0 = 10$ nm, assuming $|\delta_p| \sim 10^2$, $Q \sim 10^{12}$, gives a spin value of $S \sim 10^2$, which is significantly smaller than the spin value required for the case of a ground state particle near a Drude surface ($S \sim 10^8$). We note that this value is only limited by the quality factor of the surface resonance and can in principle be made arbitrarily small.

The spin-flip rate for the state $|a, S, m_S = 0\rangle$ in the non-retarded limit, near the plasmon resonance of the surface is given by Eq. (16)

$$\begin{aligned} \Delta\Gamma_m^{(0),\text{NR}} &\approx -\frac{3\Gamma_0\eta S(S+1)\tilde{\omega}^2}{16\tilde{z}} \text{Im} \left[\frac{(\epsilon_m - 1)}{\epsilon_m + 1} \right] \\ &\approx \frac{3\Gamma_0\eta S(S+1)\tilde{\omega}^2}{64\tilde{z}} \left(\frac{Q}{\delta_p^2} \right). \end{aligned} \quad (52)$$

For the chosen set of values, assuming $S \sim 10^2$, the decoherence rate becomes $\Delta\Gamma_m^{(0),\text{NR}} \approx 1$ MHz. We note

here that the dispersive and dissipative corrections, given by Eq. (49) and Eq. (52), contain factors of $Q/|\delta_p|$ and $Q/|\delta_p|^2$ respectively, which are characteristic of a generic coupling between a particle and a resonator [40, 85]. One can thus find a large enough quality factor Q along with a large detuning δ_p , such that the dispersive shifts can be large, without increasing the spin decoherence rate significantly.

VI. DISCUSSION

In this work, we analyze the possibility of realizing a repulsive force between a magnetic particle and a planar surface interacting via the vacuum EM field. Considering the toy model of a particle with an electric-dipole transition and a large magnetic spin, we find that as a result of the interplay between the relatively long-ranged repulsive magnetic-dipole contribution and the short-ranged attractive electric-dipole part to the total vacuum-induced force, one can possibly achieve a repulsive interaction for (i) large enough magnetizability to polarizability ratio of the magnetic particle, and (ii) in distance regimes where the ED contribution to the total force is retarded and thus weak, while the MD contribution is non-retarded and can potentially overtake the attractive ED part (see Fig. 1). We find that the level shifts induced due to the MD interaction for a ground state magnetic particle near a perfectly conducting surface contains two contributions, one that can be attributed to the broadband Casimir-Polder interaction, and a zero frequency contribution that can be understood as coming from the interaction between the static dipole and its image. Thus, we find that as a fundamental constraint for achieving near-field repulsion via MD interaction for a ground state particle near a perfectly conducting surface one requires a spin S larger than $\sim 1/\alpha$ ($\sim 10^2$), where α refers to the fine-structure constant, as in Eq. (34). In the absence of the static frequency contribution, the minimum spin value required for achieving a repulsive CP force is $\sim 1/\alpha^2$ ($\sim 10^4$), as in Eq. (31). We formulate similar conditions and estimates for achieving Casimir repulsion via MD interaction for the particle placed near surfaces described by Drude and plasma models, given by Eq. (39) and Eq. (42). We also propose some possible ways to enhance the repulsive magnetic CP interaction, such as, by preparing the particle in a superradiant state, and using surface resonances, considering particularly the level $|S, m_S = 0\rangle$. Using the analogy between the Dicke model and a spin system, similar to the enhancement in spontaneous emission, one can understand the enhancement in the magnetic CP force on the magnetic sublevel level $|S, m_S = 0\rangle$ in terms of Dicke superradiance [39].

Our results could be instructive in identifying potential systems, mechanisms, and regimes where one could realize stable levitation via repulsive magnetic-dipole induced forces. For example, we remark that the desired spin values of $S \sim 100$ are not far from the large

spin values realized for single molecular magnets (SMMs) [86, 87]. In the field of molecular magnetism, there has been a significant interest in creating single molecular complexes with magnetic spins that can be as large as $S = 105/2$ [86, 87]. For purposes of a rough estimate, assuming that an SMM with spin $S \approx 50$ constitutes roughly $N \approx 10^4$ atoms [86], such that its electric polarizability can be approximated as $\alpha_e \sim 10^4 \alpha_0$, α_0 being the single particle electric polarizability as considered earlier, and mass $M \approx 10^4$ amu, we find that such a molecule placed near a perfectly conducting surface could possibly be levitated via the magnetic-dipole interaction.

Other systems with large quantum spins such as single-domain magnetic nanoparticles [88], can potentially exhibit a macroscopic spin as large as $S \sim 10^5$. We remark that such a particle can be used to differentiate between the zero frequency response of a metal surface that is described by a Drude or a plasma model (see Eq. (40) and Eq. (43)). As shown in section IV B, the static frequency contribution being absent for the case of a Drude model, a particle with a large spin sees an MD interaction-induced force that is smaller by a factor $\sim \omega_m/(\gamma S)$ than in the case of a surface described by the plasma model.

Further, identifying collective phenomena as a potential tool to tailor vacuum forces, one can speculate using cooperative effects as a means to probe otherwise weak vacuum forces, or suppress attractive Casimir forces by preparing systems in appropriate collective states [39].

Acknowledgments

We thank Oriol Romero-Isart and Gerald E. Fux for fruitful discussions and contributions. This work was supported by the European Research Council (ERC-2013-StG 335489 QSuperMag).

Appendix A: Medium-assisted EM field

Using the macroscopic QED formalism [60, 61], the Hamiltonian for the vacuum EM field in the presence of the surface can be written as

$$H_F = \sum_{\lambda=e,m} \int d^3r \int d\omega \hbar \omega \hat{\mathbf{f}}_{\lambda}^{\dagger}(\mathbf{r}, \omega) \cdot \hat{\mathbf{f}}_{\lambda}(\mathbf{r}, \omega), \quad (\text{A1})$$

with $\hat{\mathbf{f}}_{\lambda}^{\dagger}(\mathbf{r}, \omega)$ and $\hat{\mathbf{f}}_{\lambda}(\mathbf{r}, \omega)$ as the bosonic creation and annihilation operators respectively that take into account the presence of the media. Physically these can be understood as the ladder operators corresponding to the noise polarization ($\lambda = e$) and magnetization ($\lambda = m$) excitations in the medium-assisted EM field, at frequency ω , created or annihilated at position \mathbf{r} . The medium-assisted bosonic operators obey the canonical commuta-

tion relations

$$[\hat{\mathbf{f}}_{\lambda}(\mathbf{r}, \omega), \hat{\mathbf{f}}_{\lambda'}(\mathbf{r}', \omega')] = [\hat{\mathbf{f}}_{\lambda}^{\dagger}(\mathbf{r}, \omega), \hat{\mathbf{f}}_{\lambda'}^{\dagger}(\mathbf{r}', \omega')] = 0, \quad (\text{A2})$$

$$[\hat{\mathbf{f}}_{\lambda}(\mathbf{r}, \omega), \hat{\mathbf{f}}_{\lambda'}^{\dagger}(\mathbf{r}', \omega')] = \delta_{\lambda\lambda'} \delta(\mathbf{r} - \mathbf{r}') \delta(\omega - \omega'). \quad (\text{A3})$$

The electric and magnetic field operators evaluated at the position of the particle are given as

$$\hat{\mathbf{E}}(\mathbf{r}_0) = \sum_{\lambda=e,m} \int d^3r \int d\omega \left[\bar{\bar{G}}_{\lambda}(\mathbf{r}_0, \mathbf{r}, \omega) \cdot \hat{\mathbf{f}}_{\lambda}(\mathbf{r}, \omega) + \text{H.c.} \right], \text{ and} \quad (\text{A4})$$

$$\hat{\mathbf{B}}(\mathbf{r}_0) = \sum_{\lambda=e,m} \int d^3r \int d\omega \left[\left(-\frac{i}{\omega} \right) \left[\nabla \times \bar{\bar{G}}_{\lambda}(\mathbf{r}_0, \mathbf{r}, \omega) \right] \cdot \hat{\mathbf{f}}_{\lambda}(\mathbf{r}, \omega) + \text{H.c.} \right] \quad (\text{A5})$$

respectively, where

$$[\bar{\nabla} \times \bar{\bar{G}}_{\lambda}(\mathbf{r}, \mathbf{r}', \omega)]_{il} = \epsilon_{ijk} \partial_{r_j} [\bar{\bar{G}}_{\lambda}(\mathbf{r}, \mathbf{r}', \omega)]_{kl}. \quad (\text{A6})$$

The coefficients $\bar{\bar{G}}_{\lambda}(\mathbf{r}_1, \mathbf{r}_2, \omega)$ are defined as

$$\bar{\bar{G}}_e(\mathbf{r}, \mathbf{r}', \omega) = i \frac{\omega^2}{c^2} \sqrt{\frac{\hbar}{\pi \epsilon_0} \text{Im}[\epsilon(\mathbf{r}', \omega)]} \bar{\bar{G}}(\mathbf{r}, \mathbf{r}', \omega), \quad (\text{A7})$$

$$\bar{\bar{G}}_m(\mathbf{r}, \mathbf{r}', \omega) = i \frac{\omega^2}{c^2} \sqrt{\frac{\hbar}{\pi \epsilon_0} \frac{\text{Im}[\mu(\mathbf{r}', \omega)]}{|\mu(\mathbf{r}', \omega)|^2}} \nabla \times \bar{\bar{G}}(\mathbf{r}, \mathbf{r}', \omega), \quad (\text{A8})$$

with $\epsilon(\mathbf{r}, \omega)$ and $\mu(\mathbf{r}, \omega)$ as the space-dependent permittivity and permeability, and $\bar{\bar{G}}(\mathbf{r}_1, \mathbf{r}_2, \omega)$ as the Green's tensor for a point dipole near a planar semi-infinite surface [60, 61, 65]. Since we specifically want to study the effect of the presence of surface on the particle-field interaction, assuming that the corrections from the free space Green's tensor $\bar{\bar{G}}_0(\mathbf{r}_1, \mathbf{r}_2, \omega)$ such as the Lamb shift and the free space spontaneous emission are already taken into account, we consider only the part of the field that is scattered off the surface and interacts with the dipole. This corresponds to the scattering part of the total Green's tensor defined as

$$\bar{\bar{G}}_{\text{sc}}(\mathbf{r}_1, \mathbf{r}_2, \omega) = \bar{\bar{G}}(\mathbf{r}_1, \mathbf{r}_2, \omega) - \bar{\bar{G}}_0(\mathbf{r}_1, \mathbf{r}_2, \omega). \quad (\text{A9})$$

We can thus define the interaction Hamiltonian corresponding to the interaction between the ED and MD with the part of the total EM field scattered off of the surface as

$$H_{AV}^{\text{sc}} = -\hat{\mathbf{d}} \cdot \hat{\mathbf{E}}_{\text{sc}}(\mathbf{r}_0) - \hat{\mathbf{m}} \cdot \hat{\mathbf{B}}_{\text{sc}}(\mathbf{r}_0), \quad (\text{A10})$$

where the field operators $\hat{\mathbf{E}}_{\text{sc}}(\mathbf{r}_0)$ and $\hat{\mathbf{B}}_{\text{sc}}(\mathbf{r}_0)$ are as defined in Eq. (A4) and Eq. (A5), with the total Green's tensor replaced by its scattering part ($\bar{\bar{G}}(\mathbf{r}, \mathbf{r}', \omega) \rightarrow \bar{\bar{G}}_{\text{sc}}(\mathbf{r}, \mathbf{r}', \omega)$).

Appendix B: Scattering Green's tensor near a planar surface

[60]

For a point dipole near an infinite half space, one can write the scattering Green's tensor and its double curl as

$$\bar{\bar{G}}_{\text{sc}}(\mathbf{r}_0, \mathbf{r}_0, i\xi) = \frac{1}{8\pi} \int_0^\infty \frac{dk_{\parallel} k_{\parallel}}{\kappa_{\perp}} e^{-2\kappa_{\perp} z_0} \left[-r_p(\kappa_{\perp}, i\xi) \frac{c^2}{\xi^2} \begin{pmatrix} \kappa_{\perp}^2 & 0 & 0 \\ 0 & \kappa_{\perp}^2 & 0 \\ 0 & 0 & 2k_{\parallel}^2 \end{pmatrix} + r_s(\kappa_{\perp}, i\xi) \begin{pmatrix} 1 & 0 & 0 \\ 0 & 1 & 0 \\ 0 & 0 & 0 \end{pmatrix} \right], \quad (\text{B1})$$

$$\bar{\bar{G}}_{\text{sc}}(\mathbf{r}_0, \mathbf{r}_0, i\xi) = \frac{\xi^2}{8\pi c^2} \int_0^\infty \frac{dk_{\parallel} k_{\parallel}}{\kappa_{\perp}} e^{-2\kappa_{\perp} z_0} \left[r_p(\kappa_{\perp}, i\xi) \begin{pmatrix} 1 & 0 & 0 \\ 0 & 1 & 0 \\ 0 & 0 & 0 \end{pmatrix} - r_s(\kappa_{\perp}, i\xi) \frac{c^2}{\xi^2} \begin{pmatrix} \kappa_{\perp}^2 & 0 & 0 \\ 0 & \kappa_{\perp}^2 & 0 \\ 0 & 0 & 2k_{\parallel}^2 \end{pmatrix} \right] \quad (\text{B2})$$

where $r_{s,p}$ are the Fresnel reflection coefficients for the s and p polarizations reflecting off the surface, and $\kappa_{\perp}^2 = \xi^2/c^2 + k_{\parallel}^2$. We see that all the information about the surface material is accounted for in the reflection coefficients which are given as

$$r_p(\kappa_{\perp}, i\xi) = \frac{\epsilon(i\xi) \kappa_{\perp} - \sqrt{(\epsilon(i\xi) \mu(i\xi) - 1) \xi^2/c^2 + \kappa_{\perp}^2}}{\epsilon(i\xi) \kappa_{\perp} + \sqrt{(\epsilon(i\xi) \mu(i\xi) - 1) \xi^2/c^2 + \kappa_{\perp}^2}},$$

$$r_s(\kappa_{\perp}, i\xi) = \frac{\mu(i\xi) \kappa_{\perp} - \sqrt{(\epsilon(i\xi) \mu(i\xi) - 1) \xi^2/c^2 + \kappa_{\perp}^2}}{\mu(i\xi) \kappa_{\perp} + \sqrt{(\epsilon(i\xi) \mu(i\xi) - 1) \xi^2/c^2 + \kappa_{\perp}^2}}. \quad (\text{B3})$$

Appendix C: Asymptotic potential for an particle near a metal surface

Let us consider a particle near a surface described by the Drude model with a dielectric permittivity given by Eq.(36). In the non-retarded limit, one can expand the Fresnel coefficients in Eq.(B3) to lowest order in $\sqrt{\epsilon(i\xi) - 1}\xi/(\kappa_{\perp} c)$ as

$$r_p(\kappa_{\perp}, i\xi) \approx \frac{\epsilon(i\xi) - 1}{\epsilon(i\xi) + 1} - \frac{\epsilon(i\xi) (\epsilon(i\xi) - 1)}{(\epsilon(i\xi) + 1)^2} \frac{\xi^2}{\kappa_{\perp}^2 c^2} \quad (\text{C1})$$

$$r_s(\kappa_{\perp}, i\xi) \approx -\frac{1}{4} (\epsilon(i\xi) - 1) \frac{\xi^2}{\kappa_{\perp}^2 c^2} \quad (\text{C2})$$

We can then use the above to write the electric CP potential in the non-retarded limit ($\tilde{z} \ll 1$) as

$$\tilde{U}_e^{\text{NR}} \approx -\frac{3\omega_p}{64(\sqrt{2}\omega_e + \omega_p)\tilde{z}^3}. \quad (\text{C3})$$

In the retarded limit ($\tilde{z} \gg 1$) for the electric CP interaction, one can approximate all the response functions involved (particle polarizability and the Fresnel coefficients) by their static values ($\xi \rightarrow 0$), such that, one can then simplify the electric CP potential as

$$\tilde{U}_e^{\text{R}} \approx -\frac{3}{16\pi\tilde{z}^4}, \quad (\text{C4})$$

which we can note from Table I is the same as the retarded potential for the particle near a perfectly conducting surface. This can be understood physically in terms of the fact that if the particle is far enough away from the surface such that at the typical frequencies relevant for the length scale involved the surface response effectively appears as that for a perfect conductor.

We use a similar approach to study the asymptotic behavior of the level shifts due to ED and MD interactions for the particle in different regimes, as summarized in Table I. The coefficients \mathcal{C}_j^k for Drude and plasma models used in Table I are defined as follows

$$\mathcal{C}_{e,D}^{(3)} \equiv \frac{3\omega_p}{64(\sqrt{2}\omega_e + \omega_p)}, \quad (\text{C5})$$

$$\mathcal{C}_{m,D}^{(1)} \equiv \frac{3\tilde{\omega}\eta S\omega_p}{64\omega_e} \left[\frac{\omega_p}{\omega_m + \omega_p/\sqrt{2}} + \frac{\omega_p(\omega_m + 2\gamma/\pi \ln(\gamma/\omega_m))}{2(\omega_m^2 + \gamma^2)} \right], \quad (\text{C6})$$

$$\mathcal{C}_{m,P}^{(1)} \equiv \frac{3\tilde{\omega}\eta S\omega_p}{64\omega_e} \left[\frac{\omega_p}{\omega_m + \omega_p/\sqrt{2}} + \frac{\omega_p}{2\omega_m} \right] + \frac{3}{64} \frac{\omega_p^2}{\omega_e^2} \eta S^2. \quad (\text{C7})$$

[1] P. W. Milonni, *The Quantum Vacuum: An Introduction to Quantum Electrodynamics* (Academic, San Diego,

1993).

- [2] J. D. van der Waals, *On the continuity of the gaseous and liquid states*, Thesis, Leiden, 1873.
- [3] F. London, The general theory of molecular forces, *Trans. Faraday Soc.* **33**, 8 (1937).
- [4] H. B. G. Casimir and D. Polder, The influence of retardation on the London-van der Waals forces, *Phys. Rev.* **73**, 360 (1948).
- [5] E. M. Lifshitz, The theory of molecular attractive forces between solids, *Sov. Phys. JETP* **2**, 73 (1956).
- [6] H. B. G. Casimir, On the attraction between two perfectly conducting plates, *Proc. K. Ned. Akad. Wet.* **51**, 793(1948).
- [7] Y. J. Lin, I. Teper, C. Chin, and V. Vuletić, Impact of the Casimir-Polder Potential and Johnson Noise on Bose-Einstein Condensate Stability Near Surfaces, *Phys. Rev. Lett.* **92**, 050404 (2004).
- [8] C. C. Nshii, M. Vangeleyn, J. P. Cotter, P. F. Griffin, E. A. Hinds, C. N. Ironside, P. See, A. G. Sinclair, E. Riis, and A. S. Arnold, A surface-patterned chip as a strong source of ultracold atoms for quantum technologies, *Nat. Nanotechnol.* **8**, 321 (2013).
- [9] Philipp Treutlein, David Hunger, Stephan Camerer, Theodor W. Hänsch, and Jakob Reichel, Bose-Einstein Condensate Coupled to a Nanomechanical Resonator on an Atom Chip, *Phys. Rev. Lett.* **99**, 140403 (2007).
- [10] S. Abend, M. Gebbe, M. Gersemann, H. Ahlers, H. Müntinga, E. Giese, N. Gaaloul, C. Schubert, C. Lämmerzahl, W. Ertmer, W. P. Schleich, and E. M. Rasel, Atom-Chip Fountain Gravimeter, *Phys. Rev. Lett.* **117**, 203003 (2016).
- [11] T. Nirrengarten, A. Qarry, C. Roux, A. Emmert, G. Nogues, M. Brune, J. M. Raimond, and S. Haroche, Realization of a Superconducting Atom Chip, *Phys. Rev. Lett.* **97**, 200405 (2006).
- [12] S. Pollock, J. P. Cotter, A. Laliotis, F. Ramirez-Martinez, and E. A. Hinds, Characteristics of integrated magneto-optical traps for atom chips, *New J. Phys.* **13** 043029 (2011).
- [13] Mark Keil, Omer Amit, Shuyu Zhou, David Groswasser, Yonathan Japha, and Ron Folman, Fifteen years of cold matter on the atom chip: promise, realizations, and prospects, *J. Mod. Opt.* **63**, 1840 (2016).
- [14] S. A. Meek, H. Conrad, and G. Meijer, Trapping Molecules on a Chip, *Science* **324**, 1699 (2009).
- [15] G. Sague, E. Vetsch, W. Alt, D. Meschede, and A. Rauschenbeutel, Cold-Atom Physics Using Ultrathin Optical Fibers: Light-Induced Dipole Forces and Surface Interactions, *Phys. Rev. Lett.* **99**, 163602 (2007).
- [16] E. Vetsch, D. Reitz, G. Sague, R. Schmidt, S. T. Dawkins, and A. Rauschenbeutel, Optical Interface Created by Laser-Cooled Atoms Trapped in the Evanescent Field Surrounding an Optical Nanofiber, *Phys. Rev. Lett.* **104**, 203603 (2010).
- [17] A. Goban, K. S. Choi, D. J. Alton, D. Ding, C. Lacroûte, M. Pototschnig, T. Thiele, N. P. Stern, and H. J. Kimble, Demonstration of a State-Insensitive, Compensated Nanofiber Trap, *Phys. Rev. Lett.* **109**, 033603 (2012).
- [18] J. A. Grover, P. Solano, L. A. Orozco, and S. L. Rolston, Photon-correlation measurements of atomic-cloud temperature using an optical nanofiber, *Phys. Rev. A* **92**, 013850 (2015).
- [19] V. I. Balykin, K. Hakuta, F. Le Kien, J. Q. Liang, and M. Morinaga, Atom trapping and guiding with a subwavelength diameter optical fiber, *Phys. Rev. A* **70**, 011401 (2004).
- [20] J. Vuckovic and Y. Yamamoto, Photonic crystal microcavities for cavity quantum electrodynamics with a single quantum dot, *App. Phys. Lett.* **82**, 2374 (2003).
- [21] J. D. Thompson, T. G. Tiecke, N. P. de Leon, J. Feist, A. V. Akimov, M. Gullans, A. S. Zibrov, V. Vuletić, and M. D. Lukin, Coupling a Single Trapped Atom to a Nanoscale Optical Cavity, *Science* **340**, 1202 (2013).
- [22] A. Goban, C. L. Hung, S. P. Yu, J. D. Hood, J. A. Muniz, J. H. Lee, M. J. Martin, A. C. McClung, K. S. Choi, D. E. Chang, O. Painter, and H. J. Kimble, Atom-light interactions in photonic crystals, *Nat. Comm.* **5**, 3808 (2014).
- [23] D. J. Alton, N. P. Stern, Takao Aoki, H. Lee, E. Ostby, K. J. Vahala, and H. J. Kimble, Strong interactions of single atoms and photons near a dielectric boundary, *Nat. Phys.* **7**, 159 (2011).
- [24] T. Aoki, B. Dayan, E. Wilcut, W. P. Bowen, A. S. Parkins, H. J. Kimble, T. J. Kippenberg, and K. J. Vahala, Observation of strong coupling between one atom and a monolithic microresonator, *Nature* **443**, 671 (2006).
- [25] C. L. Hung, S. M. Meenehan, D. E. Chang, O. Painter, and H. J. Kimble, Trapped atoms in one-dimensional photonic crystals, *New J. Phys.*, **15**, 083026 (2013).
- [26] R. Fermini, S. Scheel, and P. L. Knight, Trapping cold atoms near carbon nanotubes: Thermal spin flips and Casimir-Polder potential, *Phys. Rev. A* **75**, 062905 (2007).
- [27] M. S. Yeung and T. K. Gustafson, Spontaneous emission near an absorbing dielectric surface, *Phys. Rev. A* **54**, 5227 (1996).
- [28] Fam Le Kien, S. Dutta Gupta, V. I. Balykin, and K. Hakuta, Spontaneous emission of a cesium atom near a nanofiber: Efficient coupling of light to guided modes, *Phys. Rev. A* **72**, 032509 (2005).
- [29] P. Solano, P. Barberis-Blostein, F. K. Fatemi, L. A. Orozco, S. L. Rolston, Super-radiance reveals infinite-range dipole interactions through a nanofiber, *Nat. Commun.* **8**, 1857 (2017).
- [30] A. Asenjo-Garcia, J. D. Hood, D. E. Chang, and H. J. Kimble, Atom-light interactions in quasi-one-dimensional nanostructures: A Green's-function perspective, *Phys. Rev. A* **95** 033818 (2017).
- [31] S. Scheel, P. K. Rekdal, P. L. Knight, and E. A. Hinds, Atomic spin decoherence near conducting and superconducting films, *Phys. Rev. A* **72**, 042901 (2005).
- [32] P. K. Rekdal, S. Scheel, P. L. Knight, and E. A. Hinds, Thermal spin flips in atom chips, *Phys. Rev. A* **70**, 013811 (2004).
- [33] Bo-Sture K. Skagerstam, Ulrich Hohenester, Asier Eiguren, and Per Kristian Rekdal, Spin Decoherence in Superconducting Atom Chips, *Phys. Rev. Lett.* **97**, 070401 (2006).
- [34] Sahand Jamal Rahi, Mehran Kardar, and Thorsten Emig, Constraints on Stable Equilibria with Fluctuation-Induced (Casimir) Forces, *Phys. Rev. Lett.* **105**, 070404 (2010).
- [35] Kimball A. Milton, E. K. Abalo, Prachi Parashar, Nima Pourtolami, Iver Brevik, and Simen A Ellingsen, Repulsive Casimir and Casimir-Polder forces, *J. Phys. A: Math. Theor.* **45**, 374006 (2012).
- [36] Vitaly B. Svetovoy, Evanescent character of the repulsive thermal Casimir force, *Phys. Rev. A* **76**, 062102 (2007).
- [37] C. Henkel, K. Joulain, J. P. Mulet, and J. J. Greffet,

- Radiation forces on small particles in thermal near fields, *J. Opt. A: Pure Appl. Opt.* **4** (2002).
- [38] M. Antezza, L. P. Pitaevskii, S. Stringari, New asymptotic behavior of the surface-atom force out of thermal equilibrium, *Phys. Rev. Lett.* **95**, 113202 (2005).
- [39] K. Sinha, B. P. Venkatesh, and P. Meystre, Collective effects in Casimir-Polder forces, [arXiv:1803.00977v1](https://arxiv.org/abs/1803.00977v1) (2018).
- [40] D.E. Chang, K. Sinha, J.M. Taylor and H.J. Kimble, Trapping atoms using nanoscale quantum vacuum forces, *Nat. Comm.* **5**, 4343 (2014).
- [41] J. N. Munday, Federico Capasso, and V. Adrian Parsegian, Measured long-range repulsive Casimir-Lifshitz forces, *Nature* **457**, 170 (2009).
- [42] E. S. Sabisky, and C. H. Anderson, Verification of the Lifshitz Theory of the van der Waals Potential Using Liquid-Helium Films, *Phys. Rev. A* **7**, 790 (1973).
- [43] M. Ishikawa, N. Inui, M. Ichikawa, and K. Miura, Repulsive Casimir Force in Liquid, *J. Phys. Soc. Jpn.* **80**, 114601 (2011).
- [44] David A. T. Somers, and Jeremy N. Munday, Conditions for repulsive Casimir forces between identical birefringent materials, *Phys. Rev. A* **95**, 022509 (2017).
- [45] F. S. S. Rosa, D. A. R. Dalvit, and P. W. Milonni, Casimir interactions for anisotropic magnetodielectric metamaterials, *Phys. Rev. A* **78**, 032117 (2008).
- [46] L. M. Woods, D. A. R. Dalvit, A. Tkatchenko, P. Rodriguez-Lopez, A. W. Rodriguez, and R. Podgornik, Materials perspective on Casimir and van der Waals interactions, *Rev. Mod. Phys.* **88**, 045003 (2016).
- [47] Justin H. Wilson, Andrew A. Allocca, and Victor Galitski, Repulsive Casimir force between Weyl semimetals, *Phys. Rev. B* **91**, 235115 (2015).
- [48] P. Rodriguez-Lopez and A. G. Grushin, Repulsive Casimir effect with Chern insulators, *Phys. Rev. Lett.* **112**, 056804 (2014).
- [49] Michael Levin, Alexander P. McCauley, Alejandro W. Rodriguez, M. T. Homer Reid, and Steven G. Johnson, Casimir Repulsion between Metallic Objects in Vacuum, *Phys. Rev. Lett.* **105**, 090403 (2010).
- [50] T. H. Boyer, Van der Waals forces and zero-point energy for dielectric and permeable materials, *Phys. Rev. A* **9**, 2078 (1974).
- [51] O. Kenneth, I. Klich, A. Mann, and M. Revzen, Repulsive Casimir Forces, *Phys. Rev. Lett.* **89**, 033001 (2002).
- [52] V. K. Pappakrishnan, P. C. Mundru, and D. A. Genov, Repulsive Casimir force in magnetodielectric plate configurations, *Phys. Rev. B* **89**, 045430 (2014).
- [53] Timothy H. Boyer, Recalculations of Long-Range van der Waals Potentials, *Phys. Rev.* **180**, 19 (1969).
- [54] T. Datta, and L. H. Ford, Retarded van der Waals potential between a conducting place and a polarizable particle, *Phys. Lett. A* **83**, 314 (1981).
- [55] C. Henkel, B. Power, and F. Sols, New light on cavity QED with ultracold atoms, *J. Phys.: Conf. Ser.* **19**, 34 (2005).
- [56] Bo-Sture Skagerstam, Per Kristian Rekdal, and Asle Heide Vaskinn, Theory of Casimir-Polder forces, *Phys. Rev. A* **80**, 022902 (2009); Erratum *Phys. Rev. A* **86**, 049905 (2012).
- [57] H. Haakh, F. Intravaia, C. Henkel, S. Spagnolo, R. Passante, B. Power, and F. Sols, Temperature dependence of the magnetic Casimir-Polder interaction, *Phys. Rev. A* **80**, 062905 (2009).
- [58] J. J. Sakurai, *Modern quantum Mechanics*, (Addison-Wesley, 2011).
- [59] C. Cohen-Tannoudji, J. Dupont-Roc, and G. Grynberg, *Photons and Atoms: Introduction to Quantum Electrodynamics* (Wiley-VCH, 1997).
- [60] S. Y. Buhmann, *Dispersion Forces I* (Springer-Verlag, Berlin, 2012).
- [61] S. Y. Buhmann, *Dispersion Forces II* (Springer-Verlag, Berlin, 2012).
- [62] H.-P. Breuer, and F. Petruccione, *Theory of open quantum systems* (Oxford University Press, New York, 2002).
- [63] J. M. Wylie and J. E. Sipe, Quantum electrodynamics near an interface, *Phys. Rev. A* **30**, 1185 (1984).
- [64] J. M. Wylie and J. E. Sipe, Quantum electrodynamics near an interface II, *Phys. Rev. A* **32**, 2030 (1985).
- [65] T. Gruner and D. G. Welsch, Green-function approach to the radiation-field quantization for homogeneous and inhomogeneous Kramers-Kronig dielectrics, *Phys. Rev. A* **53**, 1818 (1996).
- [66] G. Barton, N. S. J. Fawcett, Quantum electromagnetics of an electron near mirrors, *Phys. Rep.* **170**, 1 (1988).
- [67] D. J. Griffiths, *Introduction to Electrodynamics* (Prentice Hall, New Jersey, 1999).
- [68] W. M. Saslow, How a superconductor supports a magnet, how magnetically ‘soft’ iron attracts a magnet, and eddy currents for the uninitiated, *Am. J. Phys.* **59**, 16 (1991).
- [69] Antoine Canaguier-Durand, Antoine Gerardin, Romain Guerout, Paulo A. Maia Neto, Valery V. Nesvizhevsky, Alexei Yu. Voronin, Astrid Lambrecht, and Serge Reynaud, Casimir interaction between a dielectric nanosphere and a metallic plane, *Phys. Rev. A* **83**, 032508 (2011).
- [70] J. E. Lennard-Jones, Processes of adsorption and diffusion on solid surfaces, *Trans. Faraday Soc.* **28**, 333 (1932).
- [71] Mark Kasperczyk, Steven Person, Duarte Ananias, Luis D. Carlos, and Lukas Novotny, Excitation of Magnetic Dipole Transitions at Optical Frequencies, *Phys. Rev. Lett.* **114**, 163903 (2015).
- [72] William M. R. Simpson, and Ulf Leonhardt, *Forces of the Quantum Vacuum: An Introduction to Casimir Physics* (Wold Scientific, London, 2015).
- [73] Michael Hartmann, Gert-Ludwig Ingold, and Paulo A. Maia Neto, Plasma versus Drude Modeling of the Casimir Force: Beyond the Proximity Force Approximation, *Phys. Rev. Lett.* **119**, 043901 (2017).
- [74] G. L. Klimchitskaya, and V. M. Mostepanenko, Casimir free energy of metallic films: Discriminating between Drude and plasma model approaches, *Phys. Rev. A* **92**, 042109 (2015).
- [75] R. S. Decca, D. López, H. B. Chan, E. Fischbach, D. E. Krause, and C. R. Jamell, Constraining New Forces in the Casimir Regime Using the Isoelectronic Technique, *Phys. Rev. Lett.* **94**, 240401 (2005).
- [76] R. S. Decca, D. López, E. Fischbach, G. L. Klimchitskaya, D. E. Krause, and V. M. Mostepanenko, Tests of new physics from precise measurements of the Casimir pressure between two gold-coated plates, *Phys. Rev. D* **75**, 077101 (2007).
- [77] C.-C. Chang, A. A. Banishev, R. Castillo-Garza, G. L. Klimchitskaya, V. M. Mostepanenko, and U. Mohideen, Gradient of the Casimir force between Au surfaces of a sphere and a plate measured using an atomic force microscope in a frequency-shift technique,

- Phys. Rev. B* **85**, 165443 (2012).
- [78] R. Castillo-Garza, and U. Mohideen, Variable-temperature device for precision Casimir-force-gradient measurement, *Rev. Sci. Instrum.* **84**, 025110 (2013).
- [79] A. A. Banishev, G. L. Klimchitskaya, V. M. Mostepanenko, and U. Mohideen, Casimir interaction between two magnetic metals in comparison with nonmagnetic test bodies, *Phys. Rev. B* **88**, 155410 (2013); Erratum *Phys. Rev. B* **89**, 159901 (2014).
- [80] A. O. Sushkov, W. J. Kim, D. A. R. Dalvit, and S. K. Lamoreaux, Observation of the thermal Casimir force, *Nat. Phys.* **7**, 230 (2011).
- [81] Daniel Garcia-Sanchez, King Yan Fong, Harish Bhaskaran, Steve Lamoreaux, and Hong X. Tang, Casimir Force and *In Situ* Surface Potential Measurements on Nanomembranes, *Phys. Rev. Lett.* **109**, 027202 (2012); Erratum *Phys. Rev. Lett.* **109**, 159902 (2012). “
- [82] R. H. Dicke, Coherence in Spontaneous Radiation Processes, *Phys. Rev.* **93**, 99 (1954).
- [83] M. Gross, and S. Haroche, Superradiance: An essay on the theory of collective spontaneous emission, *Phys. Rep.* **93**, 301 (1982).
- [84] Jingping Xu, Shenglong Chang, Yaping Yang, and M. Al-amri, Casimir-Polder force on a V-type three-level atom near a structure containing left-handed materials, *Phys. Rev. A* **93**, 012514 (2016).
- [85] Rudolf Grimm, Matthias Weidemüller, and Y. B. Ovchinnikov, Optical Dipole Traps for Neutral Atoms, *Adv. At. Mol. Opt. Phys.* **42**, 95 (2000).
- [86] Daniel Aravena, Diego Venegas-Yazigi, and Eliseo Ruiz, Exchange Interactions on the Highest-Spin Reported Molecule: the Mixed-Valence Fe₄₂ Complex, *Sci. Rep.* **6**, 23847 (2016).
- [87] M. Murugesu, M. Habrych, W. Wernsdorfer, K. A. Abboud, and G. J. Christou, Single-molecule magnets: A Mn₂₅ complex with a record $S = 51/2$ spin for a molecular species, *Am. Chem. Soc.* **126**, 4766 (2004).
- [88] Cosimo C. Rusconi, and Oriol Romero-Isart, Magnetic rigid rotor in the quantum regime: Theoretical toolbox, *Phys. Rev. B* **93**, 054427 (2016).